



DATA ARTICLE

Climate data for Odesa, Ukraine in 2021–2050 based on EURO-CORDEX simulations

Halyna Borovska¹ | Valeriy Khokhlov^{1,2}

¹Department of Meteorology and Climatology, Odessa State Environmental University, Odesa, Ukraine

²Biological and Environmental Sciences, University of Stirling, Stirling, UK

Correspondence

Halyna Borovska, Odessa State Environmental University, 15 Lvivska str., Odesa 65016, Ukraine.
Email: bga6319@gmail.com

Abstract

Climate change adaptation planning at the municipal level has become mandatory due to the increasing frequency of extreme weather and climate events. The availability of near-future climate data is the first step towards creating an adaptation plan for a city. We created the CP_OdU (Climate Projections for Odesa, Ukraine) dataset, which contains daily output variables from the 102 model runs and monthly (yearly) indices calculated for 2021–2050 in the closest to Odesa land-located model grid point. The future data are based on 26 and 76 simulations for the scenarios RCP4.5 and RCP8.5, respectively, of 14 RCMs from the EURO-CORDEX project. The horizontal resolution of spatial grids in the RCMs is $\sim 0.11^\circ$ or ~ 12 km. The CP_OdU dataset contains 76 indices relating to cloudiness, wind parameters, relative humidity, precipitation amount, snow depth and temperature. A very short description of the near-future climate in Odesa for the RCP8.5 scenario shows its trend towards a Mediterranean climate. The rising temperature supported by the change of intra-annual variations of precipitation will result in hot, dry summers and mild, moderately wet winters. The CP_OdU dataset can be used by climate scientists, applied science engineers and climate stakeholders in society for the creation of a climate change adaptation plan for Odesa, Ukraine.

KEYWORDS

EURO-CORDEX, Odesa, regional climate

Dataset Identifier: doi:10.5281/zenodo.7481942**Creator:** Valeriy Khokhlov**Title:** CP_OdU (Climate Projections for Odesa, Ukraine): Climate indices and daily meteorological variables for Odesa (Ukraine) in 2021–2050 by different RCM simulations from Euro-CORDEX**Publisher:** Zenodo**Publication year:** 2022**Resource type:** Data sets**Version:** 1.0

This is an open access article under the terms of the [Creative Commons Attribution](https://creativecommons.org/licenses/by/4.0/) License, which permits use, distribution and reproduction in any medium, provided the original work is properly cited.

© 2023 The Authors. *Geoscience Data Journal* published by Royal Meteorological Society and John Wiley & Sons Ltd.

1 | INTRODUCTION

Urban communities and infrastructure around the globe are under increasing stressors related to climate change. Kumar (2021) has described three kinds of effects of the environmental impact of extreme weather and climate events. Primary effects are changing physical systems and processes, biological systems, structure and function of ecosystems and social, economic and other development factors. Secondary effects are leading to the destruction of agriculture and infrastructure, and the contamination of the environment. Tertiary effects are responsible for the proliferation of diseases. Due to the high density of the urban population and the developed but vulnerable infrastructure, even a short-term impact of extreme weather or climatic event can have a catastrophic effect on people's well-being, not to mention the rapid proliferation of infectious diseases. In the above context, it is essential to have a strategy for climate change adaptation planning at regional and municipal levels.

According to Gu (2019), the first three natural disasters, which are highly exposed to the world's cities, are floods, droughts and cyclones—all of which are impacted by climate change. It is also well known that these events are intensifying under climate change—floods are becoming more severe, droughts and heatwaves are more prolonged and extreme, and cyclones are leading to stronger winds and heavier precipitation. The danger of natural disasters can be significantly underestimated if the climatic parameters of the recent past are even used. Therefore, the meteorological data for the near future climate must be used for climate change adaptation planning. However, the common practice for adaptation plans at the municipal level is to use inappropriate data with little consideration for predicted climate impacts or data irrelevant by spatiotemporal scale (e.g. Bonnett & Birchall, 2023).

Another important prerequisite for climate change adaptation planning at the municipal level is the existing plans at the national level and/or regional levels. Many European countries, including Ukraine, implemented National Adaptation Strategies and National Action Plans (Pietrapertosa et al., 2018). This allows the creation of a climate change adaptation plan for a city using very general, as a rule, statements from the national strategy/plan and as specific as possible meteorological data for the near future at this city.

Overpeck et al. (2011) stated two main challenges related to the data used for climate research: (i) its free availability and (ii) understandability by a broad interdisciplinary community—the former is a responsibility of climate data scientists, and the latter seems relating to the scope of climate services (Hewitt & Stone, 2021). As for the first challenge, much progress has been made

recently towards access to climate data. An example is the Copernicus Climate Change Service, implemented and supported by the European Centre for Medium-Range Weather Forecasts, where a large set of climate data (e.g. C3S, 2019) and indicators (e.g. Nobakht et al., 2019) can be freely downloaded. Success in the second challenge is harder to achieve as it requires the cooperation of climate scientists with applied science engineers and climate stakeholders in society (Lemos & Morehouse, 2005).

From the stated above, we can define the aim of this paper as to create a set of climate data and indices which is locally, spatially and timely oriented towards Odesa, Ukraine, and will be then used in climate change adaptation planning (we named the dataset CP_OdU – Climate Projections for Odesa, Ukraine). By definition, this dataset must meet the following requirements:

- should contain meteorological variables and indices that describe typical local weather conditions and extreme events for Odesa;
- should be the outcome of modelling that considers the spatial location of Odesa and has the necessary spatial resolution horizontally;
- should have a timescale that allows tracking the development of weather conditions, taking into account the uncertainties of the future climate.

The future climate of Ukraine has already been studied using different datasets (Krakovska et al., 2018, 2021; Snizhko, Shevchenko, Buznytskyi, et al., 2020; Snizhko, Shevchenko, Didovets, et al., 2020). In particular, it was found that the temperature would increase by $\sim 3.0^{\circ}\text{C}$, and precipitation would slightly decrease in Southern Ukraine, where Odesa is located, by the mid of the current century.

Probably, the EURO-CORDEX dataset (Jacob et al., 2014, 2020) is most appropriate to achieve the aim of this article. It contains many output variables that fully describe weather conditions and can be used to calculate indices defining the state of the climate and its change (e.g. Chakraborty et al., 2021; Coppola et al., 2021). The spatial resolution of the horizontal grids in the regional climate models (RCM) of the dataset is $\sim 0.11^{\circ}$ or $\sim 12\text{ km}$ allowing us to consider the features of the underlying surface in urban areas, at least on the city scale. The output variables are on the daily basis for the period up to 2,100, and the total number of simulations exceeds 100, which allows for accounting for the uncertainties of the future climate.

It is essential to use outcomes from the models with as much as a higher spatial grid resolution because daily precipitation statistics can be relatively poor (Khokhlov, 2017) if even the 25-km horizontal grid is used.

The organization of this paper is as follows. Details on the EURO-CORDEX dataset are provided in the next section. Furthermore, the climate data for Odesa obtained are presented. Finally, conclusions drawn from the present study are discussed.

The CP_OdU dataset is available at <https://doi.org/10.5281/zenodo.7481942>.

2 | DATA PROCESSING

The CORDEX was initiated to standardize modelling efforts in different regional centres with different climate models in the 14 regions worldwide—the EURO-CORDEX is the European component of the CORDEX initiative. As of December 2022, the EURO-CORDEX contains a total of 102 combinations—26 and 76 simulations for the scenarios RCP4.5 and RCP8.5, respectively (Table 1)—of 14 RCMs run at $\sim 0.11^\circ$ grid spacing with boundary conditions from eight GCMs. Output variables from these simulations were downloaded from the Copernicus Climate Change Service Climate Data Store (C3S, 2019) and the ESGF Portal at CEDA¹ (Cinquini et al., 2014).

2.1 | EURO-CORDEX dataset

Vautard et al. (2021) evaluated the EURO-CORDEX ensemble and described the quality of RCMs included in the ensemble. As they showed, the model simulations generally agree with observations and reanalyses, but there are several systematic biases as well. It should be also noted that the RCMs in the EURO-CORDEX dataset may have different horizontal grids, calendars and a set of output variables (sometimes in different units), which must be taken into account when extracting data from archives.

The CP_OdU dataset includes output variables from simulations by two scenarios—RCP4.5 and RCP8.5. The RCP4.5 scenario is a stabilization scenario, which means the radiative forcing level stabilizes at 4.5W/m^2 before 2,100 by employing technologies and strategies for reducing greenhouse gas emissions. On the other hand, in the RCP8.5 scenario, the radiative forcing level reaches 8.5W/m^2 due to increasing greenhouse gas emissions over time, that is, leading to high greenhouse gas concentration levels.

The EURO-CORDEX dataset also contains simulations for the RCP2.6 scenario. The RCP 2.6 scenario is

TABLE 1 EURO-CORDEX simulations used in this study (the number of asterisks in the upper and lower parts shows realizations for the scenarios RCP4.5 and RCP8.5, respectively).

RCM-GCM	CanESM2	CNRM-CM5	EC-EARTH	CM5-MR	MIROC5	HadGEM2-ES	ESM-LR	NorESM1-M
ALADIN53		* — *						
ALADIN63		* — *				*	*	*
ALARO0		* — *						
CCLM4-8-17	*	* — *	* — **		*	* — *	* — **	
COSMO-crCLIM		*	**			*	**	*
HadREM3		*	*			*	*	*
HIRHAM5		*	* — ***	*		* — *	*	* — *
RACMO22E		* — *	** — ***	*		* — *	*	*
RegCM4-6		*	*			*	*	*
RCA4		* — *	* — ***	* — *		* — *	* — ***	* — *
REMO2009							** — **	
REMO2015	*	*	* — *	*	*	* — *	*	* — *
WRF381H			*		*	*	*	
WRF381P		*	*	* — *		*		*

a so-called ‘peak’ scenario—the radiative forcing level reaches 3.1 W/m^2 by 2050 but returns to 2.6 W/m^2 by 2,100. However, the 3.2 W/m^2 has already been achieved by 2021 (GML, 2022)—this is why we do not consider the RCP2.6 scenario in this paper.

The complete list of output variables is quite long, but with the aim of this paper, a few of them were extracted from the dataset (Table 2).

Only two output variables from Table 2—tas and pr—can be derived from all the simulations in Table 1. Some simulations do not contain the near surface relative humidity and it can be derived by the near surface specific humidity (huss) and sea level or surface air pressure (psl or ps). Also, the snow depth can approximately be assessed by the surface snow amount, snw (kg m^{-2}). These procedures are described in Section 3.1.

The CP_OdU dataset includes the ODS-UA_RCM_outputs_day_20210101-20501231.zip file containing 102 .csv files. The names of these files follow Christensen et al. (2020) except for the element ‘VariableName_Domain’, which is replaced by the ‘ODS-UA’. For example, the file with the name ‘ODS-UA_CCCma-CanESM2_rcp85_r1i1p1_CLMcom-CCLM4-8-17_v1_day_20210101-20501231’ contains daily (‘day’) output variables from 1 January 2021 to 31 December 2050 (‘20210101-20501231’) for Odesa, Ukraine (‘ODS-UA’) from the simulation ‘v1’ by the RCM CCLM4-8-17 (‘CLMcom-CCLM4-8-17’) with the ensemble member ‘r1i1p1’ of driving GCM CanESM2 (‘CCCma-CanESM2’) for the RCP8.5 scenario (‘rcp85’). Each .csv file contains columns with the year (‘date_y’), month (‘date_m’), day (‘date_d’) and output variables (see Table 2) accessible in the simulation.

2.2 | Case-specific spatial and temporal resolution

Odesa is a port city located on the North-Western Black Sea coast (Figure 1). The location on the sea coast defines the urban mesoclimate, making it milder. The temperature during the hot summer months is somewhat lower than farther from the sea. Also, there was no permanent snow cover during some winters in the city—the snow cover boundary was situated just several tens of kilometres to the north. Sea breeze circulation that is registered in the diurnal wind change leads to an increase in humidity. Two lagoons, the Kuialnytskyi Liman and the Hadzhibeiskyi Liman, adjoin the city’s northern border and another lagoon, Sukhyi Liman, is located southwest of the city. Their location contributes to the microclimate in these areas.

The Hydrometeorological Centre of the Black and Azov Seas (HMC BAS)—the station providing the meteorological observations—is located on the elevated seacoast. The

geographic coordinates of the HMC BAS were used as a reference location to extract output variables from the EURO-CORDEX dataset. It is clear that with a horizontal grid spacing of $\sim 12\text{ km}$, the coincidence of the HMC BAS location and the grid point can only be accidental; nevertheless, the distance from the grid point to the Centre does not exceed 8.5 km. It seems logical to choose a grid point closest to the HMC BAS location, however, considering the features of the underlying surface.

Preliminary estimates have shown that the nearest to the HMC BAS grid point is often located in the Gulf of Odessa, that is, at the sea surface. From a climatological view, such a point is not an appropriate choice to describe the climate of the land. Over the sea, daily and seasonal temperature changes are less than over land. Also, the wind parameters and air humidity over the sea differ significantly from that over the land, and there is no snow cover over the sea at all. Therefore, it is better to choose the grid point closest to the HMC BAS but located on the land. Figure 1 shows that this grid point for most models is located near the western border of the city at about 9.5 km from the coastline. However, for some models—REMO2009, ALARO0, and RegCM4-6—the nearest to the Centre grid points are located directly above the urban area.

Climate research involves the analysis of long-term averages and extremes. However, data with a time resolution of a day or less is needed to obtain that values. Moreover, timescales for some climatic and weather events are significantly lesser than a month. For example, heatwaves can last several days or weeks, or start in 1 month and end in another. That is why the CP_OdU dataset contains output variables for each calendar day of 2021–2050. It

TABLE 2 Output variables from EURO-CORDEX simulations used in this study.

Name	Description	Units
clt	Total cloud fraction	%
hurs	Near surface relative humidity	%
pr	Precipitation	$\text{kg m}^{-2}\text{ s}^{-1}$
snd	Snow depth	m
sund	Duration of sunshine	s
sfcWind	Near surface wind speed	m s^{-1}
tas	Near surface air temperature	K
tasmax	Daily maximum near-surface air temperature	K
tasmin	Daily minimum near-surface air temperature	K
uas	Eastward near-surface wind	m s^{-1}
vas	Northward near-surface wind	m s^{-1}
wgsgmax	Daily maximum near-surface wind speed of gust	m s^{-1}

should be mindful of some simulations applying a ‘non-standard’ calendar year—there is no leap year, or all years are 360 days long. In the latter case, each month, including February, of the year has 30 days.

3 | DATA DESCRIPTION

3.1 | Meteorological variables

To assess the parameters of future climate as well as to calculate some indices, a set of meteorological variables is needed. With the aim of this article, this set contains meteorological variables listed in Table 3.

Here, we use the nomenclature and units defined in ECA&D (2021).

The relations between these meteorological variables and the output variables in Table 2 are quite simple and can be derived using either well-known relations (e.g. number of seconds in hour for *SS* and in day for *RR*, trigonometric ratios for *DD*, between the Celsius degree and Kelvin for *TG* etc.) or by the below formulas that are widely used in the atmospheric physics.

The RCMs’ outputs contain total cloud fraction expressed in the percentage not the cloud cover expressed in the oktas. This percentage are converted into the oktas by using an approach of Boers et al. (2010). Table 4 shows the relations between the percentage and oktas.

Some simulations do not have daily relative humidity but daily specific humidity. However, the latter can easily be recalculated into the relative humidity by relation,

$$RH = \frac{P_{H_2O}}{P_{H_2O}^*} \cdot 100\%$$

TABLE 3 Meteorological variables used in this study.

Name	Description	Units
<i>CC</i>	Daily cloud cover	oktas
<i>DD</i>	Daily value of wind direction	°
<i>FG</i>	Daily mean wind strength	m s^{-1}
<i>FX</i>	Daily maximum wind gust	m s^{-1}
<i>RH</i>	Daily relative humidity	%
<i>RR</i>	Daily precipitation amount	mm
<i>SD</i>	Daily snow depth	cm
<i>SS</i>	Daily sunshine duration	hours
<i>TG</i>	Daily mean temperature	°C
<i>TN</i>	Daily minimum temperature	°C
<i>TX</i>	Daily maximum temperature	°C

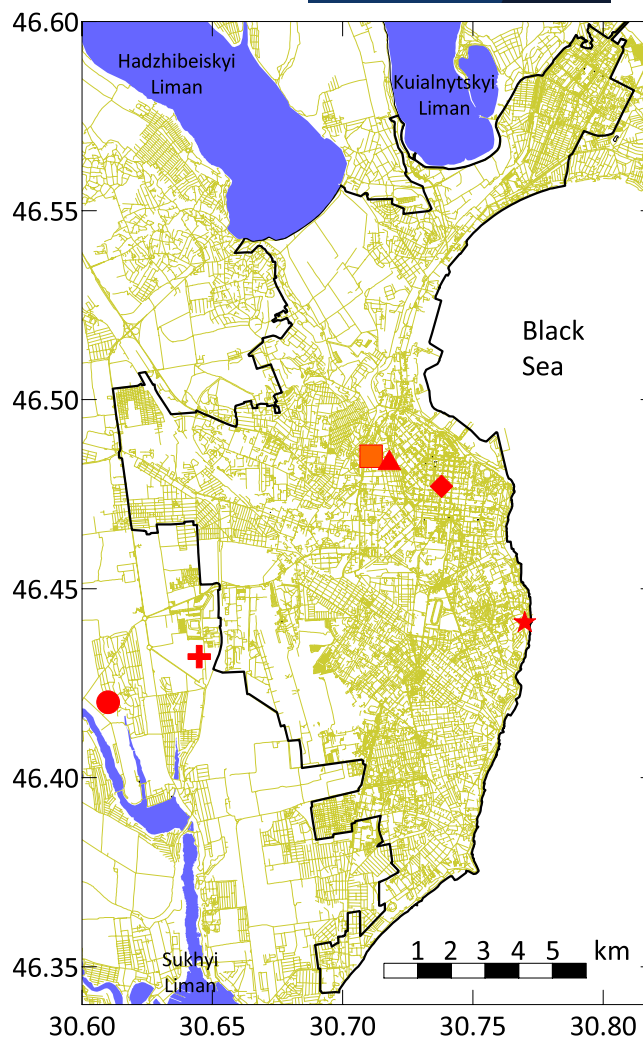


FIGURE 1 Map of Odesa with location of HMC BAS (★) and grid points by different simulations of RCMs (◆—REMO2009 and uas, vas in HadREM3, ■—ALARO0, ●—ALADIN53 and ALADIN63, ▲—RegCM4-6, +—rest models).

TABLE 4 Conversion table from cloudiness expressed in percentage to cloudiness expressed in octa (by Boers et al., 2010).

Total cloud fraction (%)	Cloud cover (oktas)
0	0
$0 < \% < 18.75$	1
$18.75 \leq \% < 31.25$	2
$31.25 \leq \% < 43.75$	3
$43.75 \leq \% < 56.25$	4
$56.25 \leq \% < 68.75$	5
$68.75 \leq \% < 81.25$	6
$81.25 \leq \% < 100$	7
100	8

where $p_{\text{H}_2\text{O}}$ is the partial pressure of water vapour

$$p_{\text{H}_2\text{O}} = \frac{p \cdot SH}{622}$$

and $p_{\text{H}_2\text{O}}^*$ is the saturated vapour pressure and regarding to Bolton (1980) can be calculated by

$$p_{\text{H}_2\text{O}}^* = 6.11 \cdot 10^{\frac{7.5t}{237.3+t}}$$

In the above equations, p is the sea level pressure (hPa), SH is the specific humidity (g kg^{-1}) and t is the air temperature ($^{\circ}\text{C}$). Let us note that some simulations provide the surface air pressure not the sea level pressure. In that case, the latter is calculated by 5 hPa increasing of surface air pressure considering the change in pressure near sea level with altitude of $\sim 1 \text{ hPa}/8 \text{ m}$ and the height of $\sim 40 \text{ m}$ above sea level for Odesa.

Simulations of some RCMs—ALADIN53, HadREM3, REMO2009, REMO2015, RegCM4-6, and WRF381P—do not have the snow depth but the surface snow amount. Then, the daily snow depth can approximately be calculated by the relation,

$$SD = 100 \cdot (0.0041 \times \text{snw} + 0.0004).$$

This linear-type relation was empirically derived by averaging the outputs from the simulations, which contain both the snow depth and surface snow amount. Figure 2 shows an example of that relationship. It can be, however, noted that the reliability of this regression equation is questionable, but it allows increasing the number of simulations for which snow cover indices are calculated. Nevertheless, end users should use the index SD resulting from that relation with care. Let us note that the HIRHAM5 RCM also used similar relation, but the coefficient before snw equals 0.0033, and the free term is zero.

3.2 | Indices

The indices used in this study are proposed in ECA&D (2021). The calculation procedure of these indices is quite simple and involves, in most cases, the calculation of the mean, minimum and maximum values of a certain meteorological variable in a certain period or the number of days where this value was above or below a certain threshold in this period of time. Table 5 contains the full list of these indices.

Odesa is a well-known tourist region in Ukraine. According to Shpak et al. (2022), Odesa has a second

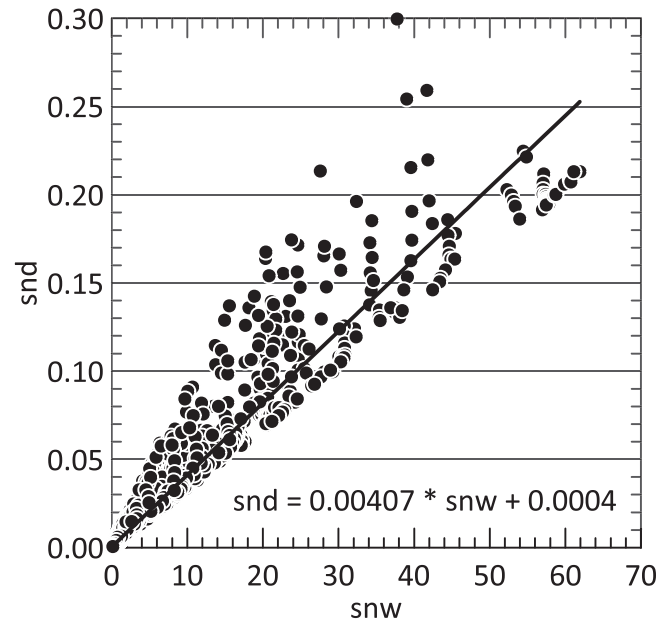


FIGURE 2 Relationship between snow depth (snd) and surface snow amount (snw) from the simulation by RACMO22E RCM with driving EC-EARTH GCM in 2021–2050 for scenario RCP 8.5.

ranking in Ukraine by recreational and tourist potential as of 2019. Considering the climate as an important factor forcing recreational and tourist potential, a few indices are involved in the database. The first index—Holiday Climate Index (HCI)—was introduced by Demiroglu et al. (2020) and allows assessing conditions for tourists from ‘dangerous’ to ‘ideal’ by the four subindices of the HCI , namely Thermal Comfort (TC), Aesthetics (A), Precipitation (P) and Wind (W), separately for urban ($HCIu$) and beach ($HCIb$) destinations by the relations

$$HCIu = 4(TC) + 2(A) + 3(P) + (W)$$

$$HCIb = 2(TC) + 4(A) + 3(P) + (W)$$

All the subindices are the table values (see Demiroglu et al., 2020).

The Odesa region is also well known in Ukraine for wine production and wine tourism with many vineyards and winery degustation sites. Therefore, the database contains two indices describing the growth of grapes—the Huglin Index (HI) and the Biologically Effective Degree Days ($BEDD$). Both indices are calculated for days from April 1 to September 30. The Huglin Index is calculated by using the daily mean and the daily maximum temperatures (Huglin, 1978)

$$HI = \sum_{01/04}^{30/09} \frac{(TG - 10) + (TX - 10)}{2} K$$

TABLE 5 Indices calculated in this study.

Acronyms	Definition of indices
CC	Mean of daily cloud cover (oktas)
CC2	Mostly sunny days (cloud cover ≤ 2 oktas) (days)
CC6	Mostly cloudy days (cloud cover ≥ 6 oktas) (days)
GD4	Growing degree days (sum of $TG > 4^{\circ}\text{C}$) ($^{\circ}\text{C}$)
GSL	Growing season length (days)
CFD	Maximum number of consecutive frost days ($TN < 0^{\circ}\text{C}$) (days)
FD	Frost days ($TN < 0^{\circ}\text{C}$) (days)
HD17	Heating degree days (sum of $17^{\circ}\text{C} - TG$) ($^{\circ}\text{C}$)
ID	Ice days ($TX < 0^{\circ}\text{C}$) (days)
CSDI	Cold-spell duration index (days)
TG10p	Days with $TG < 10$ th percentile of daily mean temperature (cold days) (days)
TN10p	Days with $TN < 10$ th percentile of daily minimum temperature (cold nights) (days)
TX10p	Days with $TX < 10$ th percentile of daily maximum temperature (cold day-times) (days)
TXn	Minimum value of daily maximum temperature ($^{\circ}\text{C}$)
TNn	Minimum value of daily minimum temperature ($^{\circ}\text{C}$)
CD	Days with $TG < 25$ th percentile of daily mean temperature and $RR < 25$ th percentile of daily precipitation sum (cold/dry days)
CW	Days with $TG < 25$ th percentile of daily mean temperature and $RR > 75$ th percentile of daily precipitation sum (cold/wet days)
WD	Days with $TG > 75$ th percentile of daily mean temperature and $RR < 25$ th percentile of daily precipitation sum (warm/dry days)
WW	Days with $TG > 75$ th percentile of daily mean temperature and $RR > 75$ th percentile of daily precipitation sum (warm/wet days)
HCIb	Holiday Climate Index: Beach
HCIb60	Days where the Holiday Climate Index: Beach ≥ 60 (good)
HCIb80	Days where the Holiday Climate Index: Beach ≥ 80 (excellent)
HCIu	Holiday Climate Index: Urban
HCIu60	Days where the Holiday Climate Index: Urban ≥ 60 (good)
HCIu80	Days where the Holiday Climate Index: Urban ≥ 80 (excellent)
CDD	Maximum number of consecutive dry days ($RR < 1$ mm) (days)
SPEI1	Standardized Precipitation Evapotranspiration Index - 1
SPEI3	Standardized Precipitation Evapotranspiration Index - 3
SPEI6	Standardized Precipitation Evapotranspiration Index - 6
SPEI12	Standardized Precipitation Evapotranspiration Index - 12
HI	Huglin Index
BEDD	Biologically Effective Degree Days
SU	Summer days ($TX > 25^{\circ}\text{C}$) (days)
TR	Tropical nights ($TN > 20^{\circ}\text{C}$) (days)
WSDI	Warm-spell duration index (days)
TG90p	Days with $TG > 90$ th percentile of daily mean temperature (warm days) (days)
TN90p	Days with $TN > 90$ th percentile of daily minimum temperature (warm nights) (days)
TX90p	Days with $TX > 90$ th percentile of daily maximum temperature (warm day-times) (days)
TXx	Maximum value of daily maximum temperature ($^{\circ}\text{C}$)
TNx	Maximum value of daily minimum temperature ($^{\circ}\text{C}$)
CSU	Maximum number of consecutive summer days ($TX > 25^{\circ}\text{C}$) (days)
RH	Mean of daily relative humidity (%)
RR	Precipitation sum (mm)
RR1	Wet days ($RR \geq 1$ mm) (days)
SDII	Simple daily intensity index (mm/wet day)
CWD	Maximum number of consecutive wet days ($RR \geq 1$ mm) (days)
R10mm	Heavy precipitation days (precipitation ≥ 10 mm) (days)
R20mm	Very heavy precipitation days (precipitation ≥ 20 mm) (days)
RX1day	Highest 1-day precipitation amount (mm)
RX5day	Highest 5-day precipitation amount (mm)
R75p	Days with $RR > 75$ th percentile of daily amounts (moderate wet days) (days)
R75pTOT	Precipitation fraction due to moderate wet days (> 75 th percentile) (%)
R95p	Days with $RR > 95$ th percentile of daily amounts (very wet days) (days)
R95pTOT	Precipitation fraction due to very wet days (> 95 th percentile) (%)
R99p	Days with $RR > 99$ th percentile of daily amounts (extremely wet days) (days)
R99pTOT	Precipitation fraction due to extremely wet days (> 99 th percentile) (%)
SD	Mean of daily snow depth (cm)

(Continues)

TABLE 5 (Continued)

Acronyms	Definition of indices
<i>SD1</i>	Snow days ($SD \geq 1$ cm) (days)
<i>SD5cm</i>	Number of days with $SD \geq 5$ cm (days)
<i>SD50cmSS</i>	Number of days with $SD \geq 50$ cm (days) Sunshine duration (hours)
<i>SSp</i>	Sunshine duration fraction with respect to daylength (%)
<i>TG</i>	Mean of daily mean temperature ($^{\circ}\text{C}$)
<i>TN</i>	Mean of daily minimum temperature ($^{\circ}\text{C}$)
<i>TX</i>	Mean of daily maximum temperature ($^{\circ}\text{C}$)
<i>DTR</i>	Mean of diurnal temperature range ($^{\circ}\text{C}$)
<i>ETR</i>	Intra-period extreme temperature range ($^{\circ}\text{C}$)
<i>vDTR</i>	Mean absolute day-to-day difference in <i>DTR</i> ($^{\circ}\text{C}$)
<i>FXc</i>	Maximum value of daily maximum wind gust (m s^{-1})
<i>FG6Bft</i>	Days with daily averaged wind ≥ 6 Bft (10.8 m s^{-1}) (days)
<i>FGcalm</i>	Calm days ($FG \leq 2 \text{ m s}^{-1}$) (days)
<i>FG</i>	Mean of daily mean wind strength (m s^{-1})
<i>DDnorth</i>	Days with northerly winds ($-45^{\circ} < DD \leq 45^{\circ}$) (days)
<i>DDsouth</i>	Days with southerly winds ($135^{\circ} < DD \leq 225^{\circ}$) (days)
<i>DDeast</i>	Days with easterly winds ($45^{\circ} < DD \leq 135^{\circ}$) (days)
<i>DDwest</i>	Days with westerly winds ($225^{\circ} < DD \leq 315^{\circ}$) (days)

where K is the function of latitude and equals 1.05 for Odesa. The Biologically Effective Degree Days index has been specifically created by Gladstones (1992) to describe grape growth and is calculated by

$$BEDD = \sum_{01/04}^{30/09} \min \left[\max \left(\frac{TX - TN}{2} - b, 0 \right), 9 \right]$$

with $b = 10$ as an appropriate value for the grapes.

ECA&D (2021) suggests calculating the Standardized Precipitation Index (Guttman, 1999) as a measure of droughts. Considering not only precipitation increase/decrease but also significant temperature increase due to global warming, Vicente-Serrano, Beguería, and López-Moreno (2010) concluded that there is an advantage in the use of drought index that includes both the precipitation and temperature and described the Standardized Precipitation Evapotranspiration Index (SPEI). In recent years, this index has been widely used and, moreover, there are global-scale interactive datasets and monitoring systems for this index (Vicente-Serrano et al., 2023; Vicente-Serrano, Beguería, López-Moreno, Angulo, & El Kenawy, 2010). In this study, we calculate the SPEI at 1-, 3-, 6- and 12-month basis using monthly mean temperature and precipitation sum for the period 1991–2050.

The calculation of some indices in Table 5 related to temperature and precipitation assumes the use of percentiles. ECA&D (2021) suggests calculating percentiles by meteorological variables of 1961–1990. From our point of view, the variables of 1991–2020 are preferable to use with the aim of this paper. This makes it possible to compare the near future climate with recent, that is, to start from

the current state when climate change adaptation planning. Figure 3 shows that the mean temperature in Odesa has increased by $\sim 1^{\circ}\text{C}$ over the past 30 years, which can result in a significant over- or underestimation of some temperature-related indices when variables of 1961–1990 are used to calculate percentiles.

Figures 3 and 4 display two commonly used climatic parameters—mean temperature and precipitation sum—for Odesa by the RCP8.5 scenario. A significant trend towards an increase in the average annual temperature will continue, and the temperature will also increase for all months. There exists only little probability of a negative average monthly temperature and only in January. Although the average annual precipitation sum will increase slightly (~ 20 mm), it will decrease significantly in summer and increase in spring and at the end of the year. In general, it seems that the climate of Odesa is moving towards the Mediterranean climate—warm to hot, dry summers and mild, moderately wet winters.

The CP_OdU dataset includes the 76 .zip files whose names contain the acronyms from Table 5. Each .zip file contains many .csv files with names, as was described earlier. Each .csv file contains indices for the months from 2021 to 2050 and an additional column with an annual mean value.

4 | CONCLUSIONS

The CP_OdU dataset contains hydrometeorological data sufficient to describe the future climate of Odesa, Ukraine. The dataset includes not only the temperature and precipitation commonly used in climate studies but

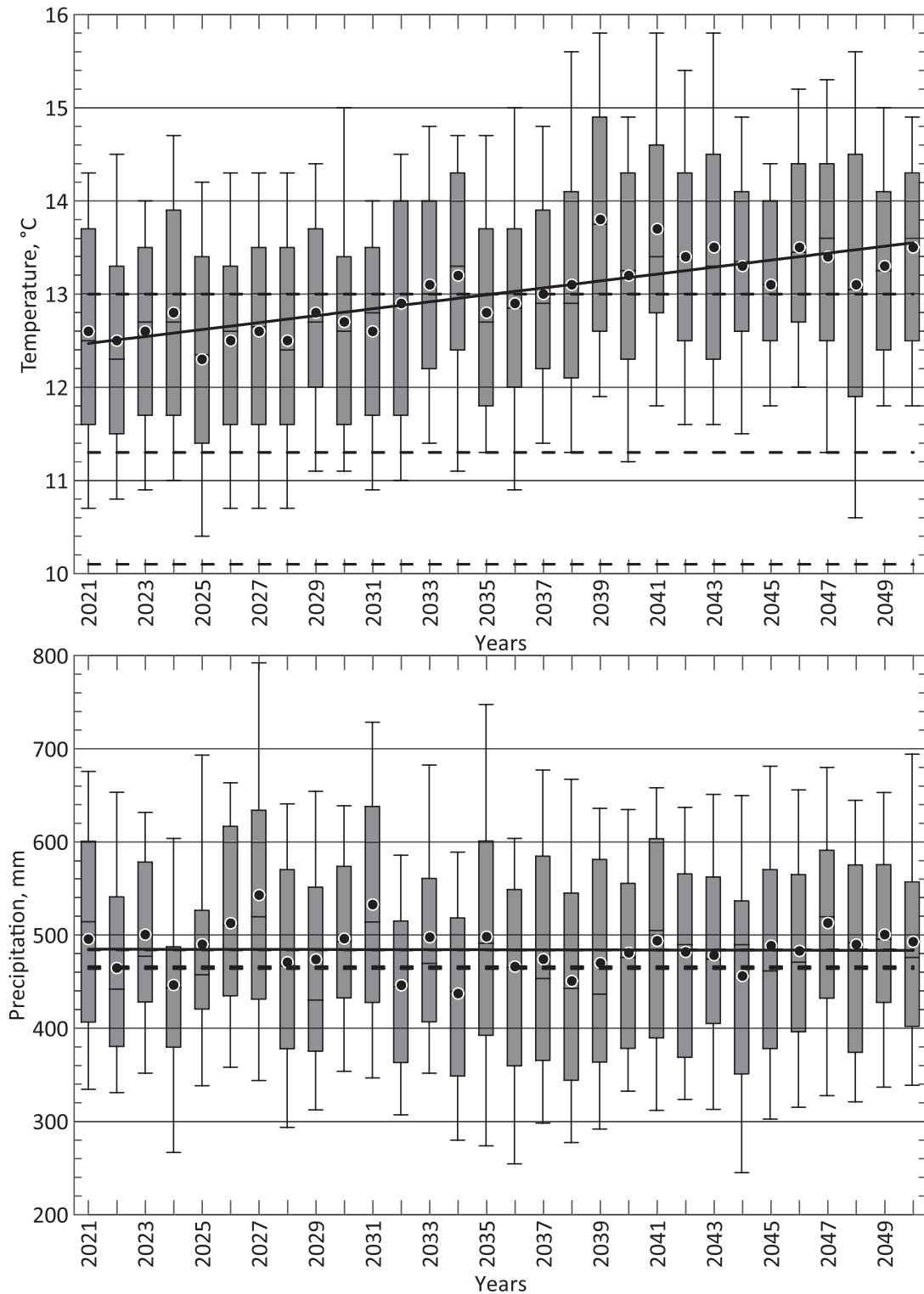


FIGURE 3 Annual mean temperature and precipitation sum in 2021–2050 for scenario RCP 8.5 in Odesa, Ukraine, by model ensemble from Table 1. The box plots visualize 10/90-percentile (whiskers), 25/75-percentile (box), median and average (dots), linear trend (solid line). The dashed lines are 30-year mean values for 1961–1990 at 10.1°C, for 1991–2020 at 11.3°C and for 2021–2050 at 13.0°C for temperature and for 1961–1990 at 464 mm, for 1991–2020 at 466 mm and for 2021–2050 at 484 mm for precipitation.

also the characteristics of cloudiness, snow cover and wind, as well as specific compound indices that could be used in different fields of the economy. The availability of climate data is although a necessary condition but only

one step towards creating a climate change adaptation plan for a city. The next steps should be to use these data to analyse the climate change impacts and to design the necessary urban engineering solutions in various fields,

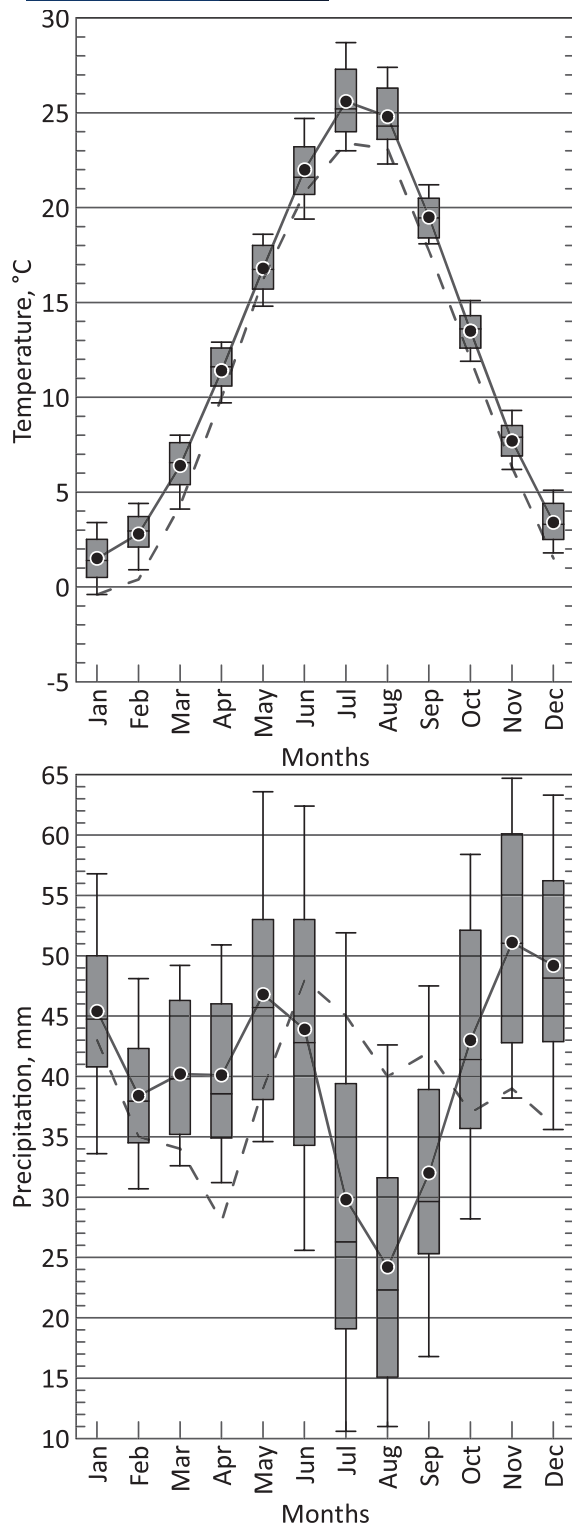


FIGURE 4 The 30-year (2021–2050) mean monthly temperature and precipitation sum for scenario RCP 8.5 in Odesa, Ukraine, by model ensemble from Table 1. The box plots visualize 10/90-percentile (whiskers), 25/75-percentile (box), median and average (dots). The dashed lines show the average values but for 1991–2020.

including farming, coastal, water, energy management etc. (e.g. El Hadri et al., 2019; Harris et al., 2023; Jenkins et al., 2023; Leone et al., 2022; Meixler et al., 2023; Pawluk De-Toledo et al., 2023; Zhou, 2023).

Before using CP_OdU dataset, bias correction of climate model simulations can be needed prior to impact studies. Bias correction is a model output statistics approach that seeks to use information from biased model outputs. A bias may be uncertainties: scenario uncertainty, model uncertainty and climate internal variability (Evin et al., 2019). Vaittinada Ayar et al. (2021) showed how important it is to maintain the climate internal variability, that is, the choice of bias correction method is essential. Tong et al. (2021) showed that the effects of bias correction are variable- and season-dependent and different methods can affect the simulated change signals differently. Thus, the bias correction process must be carefully taken.

In the case of the CP_OdU dataset, the bias correction process is a nontrivial problem since the dataset contains a lot of variables and model simulations. That is why we assume that the correct approach is to apply a bias correction before a specific impact study in some field mentioned earlier.

Finally, the CP_OdU dataset will simplify the research related to the near-future climate near Odesa, Ukraine. The format of files with data, .csv, is widely accepted by programming languages, for example, Python, or spreadsheet computer applications such as MS Excel. We also think the approach we used here can be applied to similar studies.

AUTHOR CONTRIBUTIONS

Halyna Borovska: Conceptualization (lead); data curation (supporting); methodology (equal); visualization (equal); writing – review and editing (equal). **Valeriy Khokhlov:** Conceptualization (supporting); data curation (lead); methodology (equal); visualization (equal); writing – original draft (equal).

ACKNOWLEDGEMENTS

The authors thank the two anonymous reviewers for their valuable comments and suggestions that helped improve the paper. The EURO-CORDEX data used in this work were obtained from the Copernicus Climate Change Service (C3S) Climate Data Store (<https://doi.org/10.24381/cds.bc91edc3>) and Earth System Grid Federation Portal at CEDA (<https://esgf-index1.ceda.ac.uk/search/cordex-ceda>). Valeriy Khokhlov was supported by the British Academy (No. RaR\100242).

OPEN RESEARCH BADGES



This article has earned an Open Data badge for making publicly available the digitally shareable data necessary to reproduce the reported results. The data is available at <https://doi.org/10.5281/zenodo.7481942>. Learn more about the Open Practices badges from the Center for Open Science: <https://osf.io/tvyxz/wiki>.

ORCID

Halyna Borovska  <https://orcid.org/0000-0001-9649-7661>

ENDNOTE

¹ <https://esgf-index1.ceda.ac.uk/search/cordex-ceda002F>

REFERENCES

- Boers, R., de Haij, M.J., Wauben, W.M.F., Baltink, H.K., van Ulft, L.H., Savenije, M. et al. (2010) Optimized fractional cloudiness determination from five ground-based remote sensing techniques. *Journal of Geophysical Research*, 115(24), D24116. Available from: <https://doi.org/10.1029/2010JD014661>
- Bolton, D. (1980) The computation of equivalent potential temperature. *Monthly Weather Review*, 108(7), 1046–1053. Available from: [https://doi.org/10.1175/1520-0493\(1980\)108%3C1046:TCOEPT%3E2.0.CO;2](https://doi.org/10.1175/1520-0493(1980)108%3C1046:TCOEPT%3E2.0.CO;2)
- Bonnett, N.L. & Birchall, S.J. (2023) The influence of regional strategic policy on municipal climate adaptation planning. *Regional Studies*, 57(1), 141–152. Available from: <https://doi.org/10.1080/00343404.2022.2049224>
- C3S: Copernicus Climate Change Service (C3S). (2019) CORDEX regional climate model data on single levels. *Copernicus Climate Change Service Climate Data Store (CDS)*. Available from: <https://doi.org/10.24381/cds.bc91edc3> Accessed 23 January 2023.
- Chakraborty, D., Dobor, L., Zolles, A., Hlásny, T. & Schueler, S. (2021) High-resolution gridded climate data for Europe based on bias-corrected EURO-CORDEX: the ECLIPS dataset. *Geoscience Data Journal*, 8(2), 121–131. Available from: <https://doi.org/10.1002/gdj3.110>
- Christensen, O.B., Gutowski, W.J., Nikulin, G. & Legutke, S. (2020) *CORDEX Archive Design. Version 3.2*. Available at: http://is-enes-data.github.io/cordex_archive_specifications.pdf. Accessed 23 January 2023
- Cinquini, L., Crichton, D., Mattmann, C., Harney, J., Shipman, G., Wang, F. et al. (2014) The Earth system grid federation: an open infrastructure for access to distributed geospatial data. *Future Generation Computer Systems*, 36, 400–417. Available from: <https://doi.org/10.1016/j.future.2013.07.002>
- Coppola, E., Nogherotto, R., Ciarlo', J.M., Giorgi, F., van Meijgaard, E., Kadyrov, N. et al. (2021) Assessment of the European climate projections as simulated by the large EURO-CORDEX regional and global climate model ensemble. *Journal of Geophysical Research. Atmospheres*, 126(4), e2019JD032356. Available from: <https://doi.org/10.1029/2019JD032356>
- Demiroglu, O.C., Saygili-Araci, F.S., Pacal, A., Hall, C.M. & Kurnaz, M.L. (2020) Future holiday climate index (HCI) performance of urban and beach destinations in the Mediterranean. *Atmosphere*, 11(9), 911. Available from: <https://doi.org/10.3390/atmos11090911>
- ECA&D. (2021) *European climate assessment & dataset: algorithm theoretical basis document. Version 11 from December 9, 2021*. Royal Netherlands Meteorological Institute KNMI. Available at: <https://knmi-ecad-assets-prd.s3.amazonaws.com/documents/atbd.pdf>. Accessed 23 January 2023
- El Hadri, Y., Khokhlov, V., Slizhe, M. & Sernytska, K. (2019) Wind energy land distribution in Morocco in 2021–2050 according to RCM simulation of CORDEX-Africa project. *Arabian Journal of Geosciences*, 12(24), 753. Available from: <https://doi.org/10.1007/s12517-019-4950-7>
- Evin, G., Hingray, B., Blanchet, J., Eckert, N., Morin, S. & Verfaillie, D. (2019) Partitioning uncertainty components of an incomplete ensemble of climate projections using data augmentation. *Journal of Climate*, 32(8), 2423–2440. Available from: <https://doi.org/10.1175/JCLI-D-18-0606.1>
- Gladstones, J. (1992) *Viticulture and environment: a study of the effects of environment on grapegrowing and wine qualities, with emphasis on present and future areas for growing winegrapes in Australia*. Adelaide, Australia: Winetitles.
- GML. (2022) *The NOAA annual greenhouse gas index (AGGI)*. Boulder, CO: NOAA Global Monitoring Laboratory. Available at: <https://gml.noaa.gov/aggi/aggi.html>. Accessed 23 January 2023
- Gu, D. (2019) *Exposure and vulnerability to natural disasters for world's cities*. United Nations, Department of Economics and Social Affairs, Population Division, Technical Paper No. 4. Available at: <https://www.un.org/en/development/desa/population/publications/pdf/technical/TP2019-4.pdf>. Accessed 23 January 2023
- Guttman, N.B. (1999) Accepting the standardized precipitation index: a calculation algorithm. *Journal of the American Water Resources Association*, 35(2), 311–322. Available from: <https://doi.org/10.1111/j.1752-1688.1999.tb03592.x>
- Harris, S., Mata, É., Lucena, A.F.P. & Bertoldi, P. (2023) Climate mitigation from circular and sharing economy in the buildings sector. *Resources, Conservation and Recycling*, 188, 106709. Available from: <https://doi.org/10.1016/j.resco.nrec.2022.106709>
- Hewitt, C.D. & Stone, R. (2021) Climate services for managing societal risks and opportunities. *Climate Services*, 23, 100240. Available from: <https://doi.org/10.1016/j.cliser.2021.100240>
- Huglin, M.P. (1978) Nouveau mode d'évaluation des possibilités héliothermiques d'un milieu viticole. *Comptes Rendus de l'Académie d'Agriculture*, 64, 1117–1126.
- Jacob, D., Petersen, J., Eggert, B., Alias, A., Christensen, O.B., Bouwer, L.M. et al. (2014) EURO-CORDEX: new high-resolution climate change projections for European impact research. *Regional Environmental Change*, 14(2), 563–578. Available from: <https://doi.org/10.1007/s10113-013-0499-2>
- Jacob, D., Teichmann, C., Sobolowski, S., Katragkou, E., Anders, I., Belda, M. et al. (2020) Regional climate downscaling over Europe: perspectives from the EURO-CORDEX community. *Regional Environmental Change*, 20(2), 51. Available from: <https://doi.org/10.1007/s10113-020-01606-9>
- Jenkins, L.T., Creed, M.J., Tarbali, K., Muthusamy, M., Šakić Trogrlić, R., Phillips, J.C. et al. (2023) Physics-based simulations of

- multiple natural hazards for risk-sensitive planning and decision making in expanding urban regions. *International Journal of Disaster Risk Reduction*, 84, 103338. Available from: <https://doi.org/10.1016/j.ijdr.2022.103338>
- Khokhlov, V. (2017) Climate change impact on precipitation in Odessa (Ukraine) and verification of regional modelling. *9th international workshop on precipitation in urban areas: urban challenges in rainfall analysis (UrbanRain 2012)*, 265–268
- Krakovska, S., Balabukh, V., Chyhareva, A., Pysarenko, L., Trofimova, I. & Shpytal, T. (2021) Projections of regional climate change in Ukraine based on multi-model ensembles of Euro-CORDEX. *EGU General Assembly*, 2021, EGU21-13821. Available from: <https://doi.org/10.5194/egusphere-egu21-13821>
- Krakovska, S., Palamarchuk, L., Gnatiuk, N. & Shpytal, O. (2018) Projections of air temperature and relative humidity in Ukraine regions to the middle of the 21st century based on regional climate model ensembles. *Geoinformatika*, 3(67), 62–77.
- Kumar, P. (2021) Climate change and cities: challenged ahead. *Frontiers in Sustainable Cities*, 3, 645613. Available from: <https://doi.org/10.3389/frsc.2021.645613>
- Lemos, M.C. & Morehouse, B.J. (2005) The co-production of science and policy in integrated climate assessments. *Global Environmental Change*, 15(1), 57–68. Available from: <https://doi.org/10.1016/j.gloenvcha.2004.09.004>
- Leone, A., Grassini, L. & Balena, P.P. (2022) Urban planning and sustainable storm water management: gaps and potential for integration for climate adaptation strategies. *Sustainability*, 14(24), 16870. Available from: <https://doi.org/10.3390/su142416870>
- Meixler, M.S., Piana, M.R. & Henry, A. (2023) Modeling present and future ecosystem services and environmental justice within an urban-coastal watershed. *Landscape and Urban Planning*, 232, 104659. Available from: <https://doi.org/10.1016/j.landurbplan.2022.104659>
- Nobakht, M., Beavis, P., O'Hara, S., Hutjes, R. & Supit, I. (2019) *Agroclimatic indicators from 1951 to 2099 derived from climate projections, version 1.1*. Copernicus Climate Change Service (C3S) Climate Data Store (CDS). Available from: <https://doi.org/10.24381/cds.dad6e055> Accessed 23 January 2023.
- Overpeck, J.T., Meehl, G.A., Bony, S. & Easterling, D.R. (2011) Climate data challenges in the 21st century. *Science*, 331(6018), 700–702. Available from: <https://doi.org/10.1126/science.1197869>
- Pawluk De-Toledo, K., O'Hern, S. & Koppel, S. (2023) A city-level transport vision for 2050: reimagined since COVID-19. *Transport Policy*, 132, 144–153. Available from: <https://doi.org/10.1016/j.tranpol.2022.12.022>
- Pietrapertosa, F., Khokhlov, V., Salvia, M. & Cosmi, C. (2018) Climate change adaptation policies and plans: a survey in 11 south east European countries. *Renewable and Sustainable Energy Reviews*, 81(Part 2), 3041–3050. Available from: <https://doi.org/10.1016/j.rser.2017.06.116>
- Shpak, N., Bondarenko, Y., Sroka, W., Kulyniak, I., Tsybalyta, N. & Prosovykh, O. (2022) Strategic planning of the recreational and tourism industry development: the Ukrainian evidence. *International Journal of Entrepreneurial Knowledge*, 10(1), 100–122. Available from: <https://doi.org/10.37335/ijek.v10i1.158>
- Snizhko, S., Shevchenko, O., Buznytskyi, B., Krukivska, A. & Matvienko, M. (2020) The projections of air temperature in the northern region of Ukraine following the intermediate scenario (RCP 4.5) and the high-end scenario (RCP 8.5). *XIV international scientific conference “monitoring of geological processes and ecological condition of the environment”* <https://doi.org/10.3997/2214-4609.202056035>
- Snizhko, S., Shevchenko, O., Didovets, I., Krukivska, A. & Kostyrko, I. (2020) Assessment of changes in the main climatic parameters over the territory of Ukraine during the XXI century according to scenarios based on representative concentration pathways (RCP). *XIV international scientific conference “monitoring of geological processes and ecological condition of the environment”* <https://doi.org/10.3997/2214-4609.202056032>
- Tong, Y., Gao, X., Han, Z., Xu, Y., Xu, Y. & Giorgi, F. (2021) Bias correction of temperature and precipitation over China for RCM simulations using the QM and QDM methods. *Climate Dynamics*, 57(5–6), 1425–1443. Available from: <https://doi.org/10.1007/s00382-020-05447-4>
- Vaittinada Ayar, P., Vrac, M. & Mailhot, A. (2021) Ensemble bias correction of climate simulations: preserving internal variability. *Scientific Reports*, 11, 3098. Available from: <https://doi.org/10.1038/s41598-021-82715-1>
- Vautard, R., Kadyrov, N., Iles, C., Boberg, F., Buonomo, E., Bülow, K. et al. (2021) Evaluation of the large EURO-CORDEX regional climate model ensemble. *Journal of Geophysical Research. Atmospheres*, 126(17), e2019JD032356. Available from: <https://doi.org/10.1029/2019JD032344>
- Vicente-Serrano, S.M., Beguería, S. & López-Moreno, J.I. (2010) A multiscalar drought index sensitive to global warming: the standardized precipitation evapotranspiration index. *Journal of Climate*, 23(7), 1696–1718. Available from: <https://doi.org/10.1175/2009JCLI2909.1>
- Vicente-Serrano, S.M., Beguería, S., López-Moreno, J.I., Angulo, M. & El Kenawy, A. (2010) A new global 0.5° gridded dataset (1901–2006) of a multiscalar drought index: comparison with current drought index datasets based on the palmer drought severity index. *Journal of Hydrometeorology*, 11(4), 1033–1043. Available from: <https://doi.org/10.1175/2010JHM1224.1>
- Vicente-Serrano, S.M., Domínguez-Castro, F., Reig, F., Tomas-Burguera, M., Peña-Angulo, D., Latorre, B. et al. (2023) A global drought monitoring system and dataset based on ERA5 reanalysis: a focus on crop-growing regions. *Geoscience Data Journal*. in Press. Available from: <https://doi.org/10.1002/gdj3.178>
- Zhou, Y. (2023) Climate change adaptation with energy resilience in energy districts – a state-of-the-art review. *Energy and Buildings*, 279, 112649. Available from: <https://doi.org/10.1016/j.enbui.2022.112649>

How to cite this article: Borovska, H. & Khokhlov, V. (2023) Climate data for Odesa, Ukraine in 2021–2050 based on EURO-CORDEX simulations. *Geoscience Data Journal*, 00, 1–12. Available from: <https://doi.org/10.1002/gdj3.197>